Anisotropic normal-state properties of the MgB_2 superconductor

2005 J. Phys.: Condens. Matter 17 965

(http://iopscience.iop.org/0953-8984/17/6/014)

INSTITUTE OF PHYSICS PUBLISHING JOURNAL OF PHYSICS: CONDENSED MATTER

J. Phys.: Condens. Matter **17** (2005) 965–978 doi:10.1088/0953-8984/17/6/014

Anisotropic normal-state properties of the MgB_2 superconductor

Pablo de la Mora[1], Miguel Castro[2] and Gustavo Tavizon[2]

[1] Departamento de Física, Facultad de Ciencias, UNAM, Ciudad Universitaria 04510, Coyoacán, DF, Mexico
[2] Departamento de Física y Química Teórica, Facultad de Química, UNAM, Ciudad Universitaria, Coyoacán 04510, DF, Mexico

E-mail: delamora@servidor.unam.mx

Received 28 May 2004, in final form 9 December 2004
Published 28 January 2005
Online at stacks.iop.org/JPhysCM/17/965

Abstract

Based on the experimentally-found existence of two superconducting gaps in MgB_2 (one gap associated to the boron σ-states and the other to the boron π-states), the different contributions to the transport properties, electrical conductivity and Hall coefficient were studied using the full potential-linearized augmented plane wave method and the generalized gradient approximation. Four different relaxation times were needed to adjust the electrical conductivity and Hall coefficient to experimental values. MgB_2 doping was analysed in the *rigid band approximation*; this permitted a detailed study of the partial substitution of magnesium for aluminium ($Mg_{1-x}Al_xB_2$). Other substitutions such as AB_2 (A = Be, Sc, Zr, Nb and Ta) are also discussed. The MgB_2 σ-bands (boron σ-states), which are associated to the large gap, are very anisotropic at E_F, while the π bands have very little anisotropic character. In $Mg_{1-x}Al_xB_2$, T_c diminishes with Al content; the other compounds are not superconductors or have a low T_c. In this work it was found that with electron doping, such as Al substitution, the σ-band conductivity decreases and the corresponding bands become less anisotropic. The σ-band contribution for BeB_2 and ScB_2 at E_F is very small and the anisotropy is much lower. For Zr, Nb and Ta there are no σ-bands at E_F. These results give a clear connection between superconductivity and the character of the σ-band, band conductivity, and band anisotropy. This gives a plausible explanation for the diminution of T_c with different doping of MgB_2.

(Some figures in this article are in colour only in the electronic version)

Dedicated to John B Goodenough ('Prof') on the occasion of his 82nd anniversary.

1. Introduction

Soon after superconductivity was discovered in MgB_2, the strong anharmonicity of the boron in-plane phonons was found. These anharmonic vibrations were originally proposed as one of the possible explanations for the high transition temperature in this compound (Yildirim *et al* 2001). Another possibility was the influence of the two-dimensional character exhibited by the crystal structure on the electronic patterns (Nature 2001), but electronic structure calculations (Satta *et al* 2001, de la Mora *et al* 2002) and experimental measurements (Masui and Tajima 2003) showed that this material is essentially a bulk conductor with a ratio of 1–10 (the theoretical value is $\approx$1 and the experimental one is $\approx$3–10) for the anisotropy in the electrical conductivity in the a/c-directions. Soon after, MgB_2 produced more surprises; Liu *et al* (2001) found theoretical evidence that there should be two superconducting gaps. One of them is associated to the $p_{x,y}$-orbitals (σ-bands): these σ-orbitals have a high a/c anisotropy; the other gap, associated to B:p_z and Mg-orbitals, has a three-dimensional character. The existence of two gaps has been experimentally confirmed through tunnelling spectra (Eskildsen *et al* 2002, Iavarone *et al* 2002, Schmidt *et al* 2002, Szabó *et al* 2001). In this paper the dimensionality of the different σ and π bands is studied by *density functional theory* (DFT). The σ-bands were found to be highly anisotropic, while the π-bands were found to be essentially three-dimensional. The band contributions, two of σ-character and two of π-character, were analysed separately with different relaxation times. By trying to reconcile the experimental and theoretical results it was possible to define relative relaxation time values. Finally, with these relaxation-time values it was possible to have a complete theoretical description of the experimental results.

Using the *rigid band approximation* the separate σ-band and π-band contributions to the electrical conductivity and the Hall coefficient are discussed as function of electron doping in $Mg_{1-x}Al_xB_2$. The compounds BeB_2 and ScB_2 are analysed as a function of the anisotropy and the in-plane conductivity of the σ-bands. For ZrB_2, NbB_2 and TaB_2 the excess of d-electrons provided by the Zr, Nb and Ta atoms fills up and perturbs the anisotropic σ-boron bands, therefore destroying the high-T_c superconductivity.

2. Computational procedure

The electronic structure calculations were done using the *WIEN2k* code (Blaha *et al* 2001), which is a full potential-linearized augmented plane wave (FP-LAPW) method based on DFT. The generalized gradient approximation of Perdew *et al* (1996) was used for the treatment of the exchange–correlation interactions. The energy threshold to separate localized and non-localized electronic states was -6 Ryd. For the number of plane waves the used criterion was R_{MT}^{min}(muffin tin radius) $\times$ K_{max} (for the plane waves) $= 9$. The number of k-points used was $19 \times 19 \times 15$ (320 in the irreducible wedge of the Brillouin zone). The muffin-tin radius for magnesium is 1.8 a_0 and for boron it is 1.68 a_0 (a_0 is the Bohr radius). The charge density criterion with a threshold of 10^{-4} was used for the convergence. A denser mesh of $100 \times 100 \times 76$ (34 476 in the irreducible wedge) was used for the evaluation of the electrical conductivity and the Hall coefficients.

3. Crystal and electronic structure

The crystal structure of MgB_2 is composed of alternating planes of boron and magnesium. The boron planes have a honeycomb arrangement (like graphite but with no displacement) and between two contiguous planes there are the Mg atoms on the line passing through the

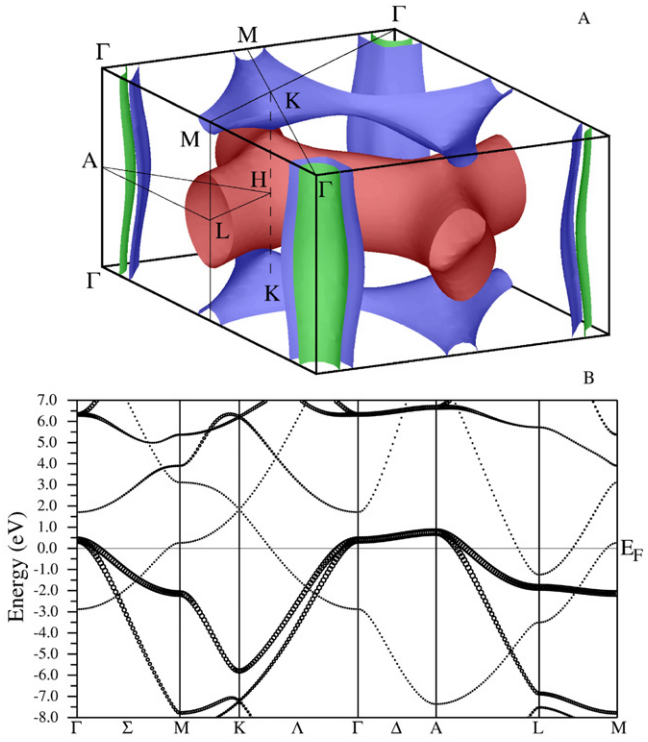

Figure 1. (A) Fermi surface of MgB_2 (Kortus *et al* 2001). (B) Band structure of MgB_2. Γ–M–K–Γ and A–L correspond to the ab-plane directions and Γ–A and L–M to the c-direction. The bands with large circles are of σ-character, while the ones with dots are of π-character.

centre of the boron hexagons, that is, Mg atoms form a hexagonal arrangement. MgB_2 has the so-called AlB_2 structure ($P6/mmm$, space group 191), with $a = 3.0864$ Å, $c = 3.5215$ Å.

The band structure at E_F largely reflects the crystal symmetry, which can be clearly seen from the Fermi surface structure (figure 1(A)) and band structure (figure 1(B)): there are two almost-vertical surfaces around and close to the Γ–A line; their distance is less than 0.31 of the Γ–M distance. The corresponding bands are mainly of B:$p_{x,y}$ character, having almost no magnesium contribution (σ-bands). These bands have little slope in the c-direction (Γ–A and L–M) while in the plane (Γ–M–K–Γ and A–L) the slope is large. The corresponding electrical conductivity, as we will prove, should be mainly in the ab-plane, being almost insulating in the c-direction.

There are another two Fermi surfaces forming a horizontal honeycomb-like tubular surfaces, with the holes around the Γ–A line; the separation to this line is more than 0.80 the Γ–M distance. One of the surfaces lies in the Γ–M–K plane, surrounding the M–K line; the other is in the A–L–H plane and surrounds the L–H line. The corresponding bands are formed by B:p_z with a small magnesium contribution (de la Mora *et al* 2002) (π-bands); these bands are three-dimensional or bulk-like, with a large slope at E_F in all directions.

Since the Fermi surfaces can be easily separated in k-space the corresponding contribution to the transport properties can also be independently calculated; in the *relaxation time approximation* the transport properties (conductivity and Hall coefficient) depend on the band structure at E_F only (Allen *et al* 1987).

4. Conductivity and Hall coefficient expressions

Within the framework of the *relaxation time approximation* the transport properties, for one band (n), can be estimated from band structure results, using the following expressions: (de la Mora *et al* 2002, Allen *et al* 1987, Hamada *et al* 1990).

$$\sigma^n_{\alpha\beta} = \frac{e^2\tau^n(\varepsilon_F, T)}{\Omega_0}\int \mathrm{d}^3k\, v^n_\alpha(k)v^n_\beta(k)\delta(\varepsilon_F - \varepsilon(k))$$
$$= \frac{e^2\tau^n}{\hbar\Omega_0}\int \mathrm{d}A_\alpha \sum_i S(v^{ni}_\alpha(k_F))v^{ni}_\beta(k_F) \tag{1}$$

$$\sigma^n_\alpha \equiv \sigma^n_{\alpha\alpha} = \frac{e^2\tau^n}{\hbar\Omega_0}\int \mathrm{d}A_\alpha \sum_i |v^{ni}_\alpha(k_F)| \tag{1a}$$

$$\sigma^n_{H\gamma} \equiv \sigma^n_{H\alpha\beta\gamma} = \frac{(e\tau^n)^2}{\hbar\Omega_0}\int \mathrm{d}^3k v^n_\alpha(k)[v^n(k)\times\nabla_k]_\gamma v^n_\beta(k)\delta(\varepsilon(k)-\varepsilon_F)$$
$$= \frac{(e\tau^n)^2}{\hbar^2\Omega_0}\int \mathrm{d}A_\alpha \sum_i S(v^n_\alpha(k_F))\left[v^n_\alpha(k_F)\frac{\mathrm{d}v^n_\beta}{\mathrm{d}k_\beta}\bigg|_{k_F} - v^n_\beta(k_F)\frac{\mathrm{d}v^n_\beta}{\mathrm{d}k_\alpha}\bigg|_{k_F}\right] \tag{2}$$

where the summation over i runs over all the crossings at the Fermi energy of band n. Here τ^n is the relaxation time, Ω_0 is the normalization volume, $S(v^n_\alpha(k_F))$ is the sign of $v^n_\alpha(k_F)$ and $\mathrm{d}^3k = \mathrm{d}A_\alpha\,\mathrm{d}k_\alpha$, where A_α is the area perpendicular to k_α. The second line of equations (1) and (2) is obtained from the properties of the delta function, and from them $\sigma^n_{\alpha\beta}$ and $\sigma^n_{H\alpha\beta\gamma}$ can be easily calculated.

In expressions (1) and (2) $\sigma^n_{\alpha\beta}$ is the conductivity and $\sigma^n_{H\alpha\beta\gamma}$ the Hall conductivity (note that the symbol σ without subscripts is used to refer to bands). Due to the Onsager relations, $\sigma_{H\alpha\beta\gamma} = -\sigma_{H\beta\alpha\gamma}$, and the crystal's hexagonal symmetry only two terms are independent: $\sigma_{Hayc}(\equiv\sigma_{Hc})$ and $\sigma_{Hyca} = \sigma_{Hcay}(\equiv\sigma_{Ha})$, where the last subscript is the direction of the magnetic field (α, β and γ are perpendicular axes in $\sigma^n_{H\alpha\beta\gamma}$ and y is the axis perpendicular to a on the plane).

The simplest extension to many bands is (Schulz *et al* 1992b, Ashcroft and Mermin 1976)

$$\sigma_{\alpha\beta} = \sum_n \sigma^n_{\alpha\beta}$$
$$\sigma_\alpha = \sum_n \sigma^n_\alpha \tag{3}$$
$$\sigma_{H\gamma} = \sum_n \sigma^n_{H\gamma}.$$

In terms of equations (1)–(3) the Hall coefficient is (Allen *et al* 1987, Hamada *et al* 1990)

$$R_{H\gamma} = \frac{\sigma_{H\gamma}}{\sigma_\alpha\sigma_\beta}. \tag{4}$$

The solution for R_H is not constrained by a variational principle, so it should be regarded as qualitatively and not a quantitatively adequate model (Schulz *et al* 1992b). Nevertheless the R_H calculations of Allen and Schulz (1993) for ReO_3 were within 30% of the experimental data; Schulz *et al* (1992a) using calculated *CPA*-values of Butler (1984) had a very good qualitative (almost quantitative) agreement with experimental values.

As can be seen from equations (1) and (2) the conductivity and the Hall coefficient can be calculated, except for τ^n, from the band structure. Note that τ^n contains all the temperature dependence, except for the temperature smearing at the Fermi energy, which was approximated

to a δ-function (Allen *et al* 1988). At higher level of approximation additional anisotropy enters from the anisotropy of scattering, but from the cases studied by Allen and co-workers (Allen 1987, Allen *et al* 1986, 1988) this turns out to be a surprisingly small effect (a few per cent), at least for electron–phonon scattering at $T \geqslant \theta_D$.

Since the terms σ_α^n/τ^n ($\equiv\delta_\alpha^n$) and $\sigma_{\mathrm{H}\alpha}^n/(\tau^n)^2$ ($\equiv\delta_{\mathrm{H}\alpha}^n$) play an important role, they will be called conductivity factor and Hall conductivity factor. The conductivity σ_α^n is related to the plasma frequency (w_{p}^n) and to the Fermi velocity (v_{F}^n) by (Allen *et al* 1987, 1988, Ashcroft and Mermin 1976)

$$\delta_\alpha^n \equiv \frac{\sigma_\alpha^n}{\tau^n} = \frac{(w_{p\alpha}^n)^2}{4\pi} = e^2 N(\varepsilon_{\mathrm{F}})(v_{F\alpha}^n)^2, \tag{5}$$

where $N(\varepsilon_{\mathrm{F}})$ is the density of states. With the use of this equation the expression for the conductivity σ_α is in agreement with that found by Mazin and Antropov (2003), whose expressions are beyond LOVA (lowest-order variational approximations, Pinski *et al* 1981).

5. Results and discussion

Regarding the problem of the anisotropic character observed in the band structure of MgB_2 and its consequences on the normal state transport properties of this intermetallic compound, there is a simple and intuitive relation arising from the conductivity expression (equation (1*a*)). Besides the *relaxation time*, there are two contributions to conductivity in such equation; one of them is the area vector $\boldsymbol{dA}$ (which is on the Fermi surface), and the other one is $\boldsymbol{v}$ ($=\hbar^{-1}\nabla_k\varepsilon$) at the neighbourhood of the Fermi level. Since both $\boldsymbol{dA}$ and $\boldsymbol{v}$ are parallel vectors, then $v_a/v_c = \mathrm{d}A_a/\mathrm{d}A_c$; therefore $\mathrm{d}\sigma_a^n/\mathrm{d}\sigma_c^n = v_a\,\mathrm{d}A_a/v_c\,\mathrm{d}A_c = (\mathrm{d}A_a/\mathrm{d}A_c)^2 = (v_a/v_c)^2$. This expression does not hold for the integrated conductivities, σ_a^n/σ_c^n, but it should be approximate for simple surfaces:

$$\frac{\sigma_a^n}{\sigma_c^n} \approx \frac{v_a^2}{v_c^2} \approx \frac{A_a^2}{A_c^2}, \tag{6}$$

where A_α is the Fermi surface area seen from the α-direction, σ_α^n is the conductivity of band n in the same direction and v_α^n is the maximum velocity in each direction, which usually falls in a k-point of the Fermi surface crossed by the band-structure plots. This expression (6) is exact for the Fermi surface of parabolic bands ($\varepsilon = k_x^2/d^2 + k_y^2/e^2 + k_z^2/f^2$).

Expression (6) gives an intuitive feeling about the anisotropy of the conductivity for a given band; that is, the asymmetry can be estimated by observing the geometry of the Fermi surface or by comparing the slope of the involved bands in different directions. For example, for the case of the MgB_2 bands taken individually the ratio $(\sigma_a/\sigma_c)/(A_a/A_c)^2$ is very close to unity, between 0.83 and 1.04, this is not only at E_{F} but in the energy range $[-1.2, 1.5\ \mathrm{eV}]$ (see the *rigid band approximation* in section 5.2). For all four bands together, with $\tau^n = \tau$, it deviates more (0.89–1.8) and this is due to the different character of the σ- and π-bands. This shows that for simple Fermi surfaces expression (6) seems to be a good estimate.

Now, we use this expression to analyse MgB_2; the σ-Fermi surfaces have a tubular form (figure 1(A)), therefore seen from above (c-direction) a small area is displayed in the form of a ring, while from the perpendicular direction (ab-plane) a much larger area is spanned. Therefore a very anisotropic conductivity results from these Fermi surfaces. On the other hand the π-surfaces display a large area in all directions and their associated contribution to conductivity should be quite isotropic.

Table 1. Conductivity factors (columns 2 and 3) and Hall conductivity factors (columns 4 and 5) in the a- and c-directions and for all bands in MgB_2. Arbitrary units are used.

	Conductivity		Hall	
δ	a	c	a	c
$\sigma 1$	0.197	0.0038	0.028	1.99
$\sigma 2$	0.198	0.0055	0.022	0.86
$\pi 1$	0.203	0.475	1.86	0.28
$\pi 2$	0.500	0.498	−2.88	0.88

5.1. Relaxation times τ

As mentioned above, the Fermi surfaces can be easily separated in k-space, therefore the conductivity can be calculated for each of the bands independently. There are four bands at E_F, two σ-bands ($\sigma 1$ and $\sigma 2$) and two π-bands ($\pi 1$ and $\pi 2$). From the band structure plots it can be deduced that $\sigma 1$ (lower in energy) is the one closer to the Γ–A line (see for example Γ–M in figure 1(B)) and $\pi 1$ (lower in energy) is in the Γ–K–M plane (K–M in figure 1(A)).

Using equations (1a) and (2) for the separate bands the conductivity factor and Hall conductivity factor for MgB_2 were calculated; the relative values are shown in table 1.

We have found only two experimental reports for σ_c in the literature, Eltsev *et al* (2003) and Masui *et al* (2002). Only Eltsev *et al* (2003) reports both conductivity and Hall coefficient measurements: they find for the conductivity ratio (CR) $\sigma_a/\sigma_c \approx [3.4, 3.6]$, and that this ratio is almost temperature independent; for the Hall conductivity ratio (HCR) they find $\sigma_{Ha}/\sigma_{Hc} \approx [-0.3, -0.8]$.

Masui and Tajima (2003) claim that since MgB_2 preferentially grows along ab-directions, the thickness of a single crystal along the c-axis has not been enough for accurate out-of-plane transport measurements; the measurements give a CR between 3 and 10.

Using the values of table 1 and with only one relaxation time ($\tau^n = \tau$) then CR = 1.12 and HCR = −0.275. This is incompatible with the experimental results (see figure 2(A)), therefore it is necessary to have a more flexible model. A first improvement can be achieved by having two relaxation times: τ^σ (for the σ-bands) and τ^π (for the π-bands). Using equations (3)–(5), then HCR versus CR can easily be calculated using the values of table 1. Now there is an extra degree of freedom and the possible values form a curve; this is shown in the top line (2τ) of figure 2(A). This curve is still far from the experimental values.

As mentioned above, the Hall conductivity expression (equation (2)) is correct within 30% of the experimental data (Allen and Schulz 1993); with this in mind the components of the HCR, $\delta^n_{H\alpha}$ (equation (3)), were adjusted by 30% and 60% to try to fit the experimental values (figure 2(A)). These large adjustments still do not come close to the experimental values.

Since two relaxation times are not enough to fit the experimental date within the 30% error then a further improvement is to have separate relaxation times τ^n for each band. These relaxation times will be parameterized by x, y and z:

$$\begin{array}{lll} \tau^{\sigma 1} = (1-x)\tau^\sigma & \tau^{\sigma 2} = x\tau^\sigma & \tau^\sigma = (1-z)\tau \\ \tau^{\pi 1} = (1-y)\tau^\pi & \tau^{\pi 2} = y\tau^\pi & \tau^\pi = z\tau \end{array} \qquad (7)$$

where $0 \leqslant x, y, z \leqslant 1$. With this parameterization τ cancels in CR and HCR and only three free parameters (x, y and z) remain to adjust the experimental values. Since the experimental CR is almost temperature independent (Eltsev *et al* 2003), then, from equation (3), τ^σ/τ^π should also be temperature independent; therefore the only temperature dependence should be on τ, and not on x, y or z.

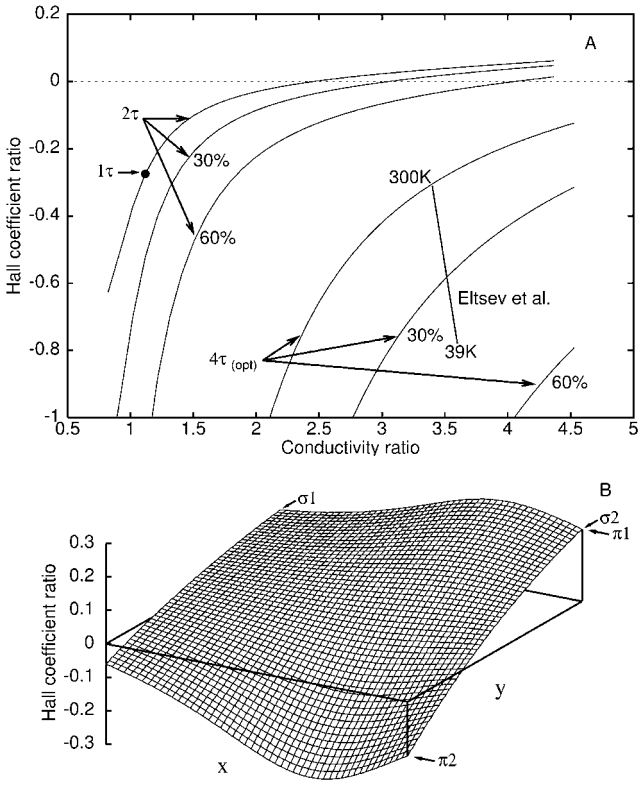

Figure 2. (A) Hall coefficient ratio (HCR) R_{Ha}/R_{Hc} versus conductivity ratio (CR) σ_a/σ_c. The vertical line shows the experimental values (Eltsev *et al* 2003). The point at (1.12, −0.275), 1τ, is for one relaxation time $\tau^n = \tau$. The top curve, 2τ, is for two relaxation times (τ^σ and τ^π); the two lines below have 30% and 60% adjustments (these curves are only drawn on the side of the experimental values). The following three curves, $4\tau_{(opt)}$, give the optimized HCR (see the text): the top one is without correction, the others are for 30% and 60% corrections. (B) HCR versus x and y for CR = 3.5 (see the text). Note that from equation (7), $x \approx 0$ implies $\tau^{\sigma 1} \gg \tau^{\sigma 2}$, $x \approx 1$ implies $\tau^{\sigma 1} \ll \tau^{\sigma 2}$; the same holds for y, $\tau^{\pi 1}$ and $\tau^{\pi 2}$.

The experimental CR value of Eltsev *et al* (2003), 3.5, can be taken into account to eliminate z, and the HCR can now be plotted as a function of x and y; this is shown in figure 2(B). In most of the x and y ranges the theoretical HCR value is positive; only for values $y \approx 1$ it is negative. The experimental HCR values are in the range from −0.3 to −0.8; this implies $\tau^{\pi 2} \gg \tau^{\pi 1}$, and the minimum in figure 2(B) is at $x \approx 2/3$ ($\tau^{\sigma 2} \approx 2\tau^{\sigma 1}$), $y \approx 1$.

Using these new optimized values, $x \approx 2/3$, $y \approx 1$, the HCR can now be plotted as a function of z, or even better as a function of the CR. This curve is shown in figure 2(A) as $4\tau_{(opt)}$. As was done for the two relaxation times, τ^σ and τ^π, the $\delta^n_{H\alpha}$ within the HCR can be also modified by 30% and 60%. The corresponding curves are shown in figure 2(A) below the $4\tau_{(opt)}$ curve. Now the high temperature values of Eltsev *et al* (2003) (CR = 3.4, HCR = −0.3) are reproduced. The low temperature values (CR = 3.6, HCR = −0.8) are within ≈ 40% correction.

In figure 2(B) the variation of the HCR with x is not as drastic as with y and other $\tau^{\sigma 2}$:$\tau^{\sigma 1}$ ratios (that is, $x \neq 2/3$) could approximately reproduce the CR, HCR experimental values, in particular $x = \frac{1}{2}$; that is, $\tau^{\sigma 1} = \tau^{\sigma 2} (= \tau^\sigma/2)$.

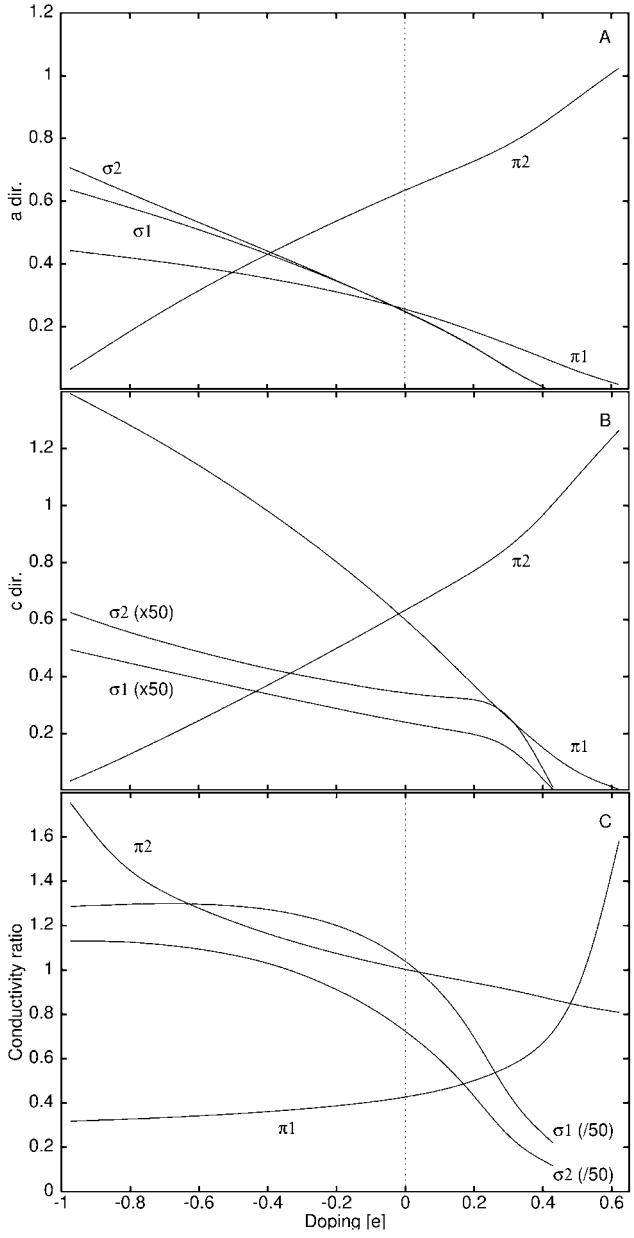

Figure 3. Conductivity factors (δ_γ^n) of different bands: (A) a-direction, (B) c-direction and (C) a/c-ratio. The σ-band contribution is very small in the c-direction, therefore the values in (B) are multiplied by 50 and in (C) they are divided by 50.

It is worth noticing that having one relaxation time for the σ-bands and two for the π-bands would reflect, on one hand, the very similar behaviour of the $\sigma 1$- and $\sigma 2$-bands and, on the other hand, the quite different behaviour of the $\pi 1$- and $\pi 2$-bands (see figures 3 and 4).

Putti *et al* (2003b) found values of thermal conductivity relaxation times; τ_Q^σ and τ_Q^π (these are related to the electrical conductivity values, τ^σ and τ^π, and in LOVA they are equal,

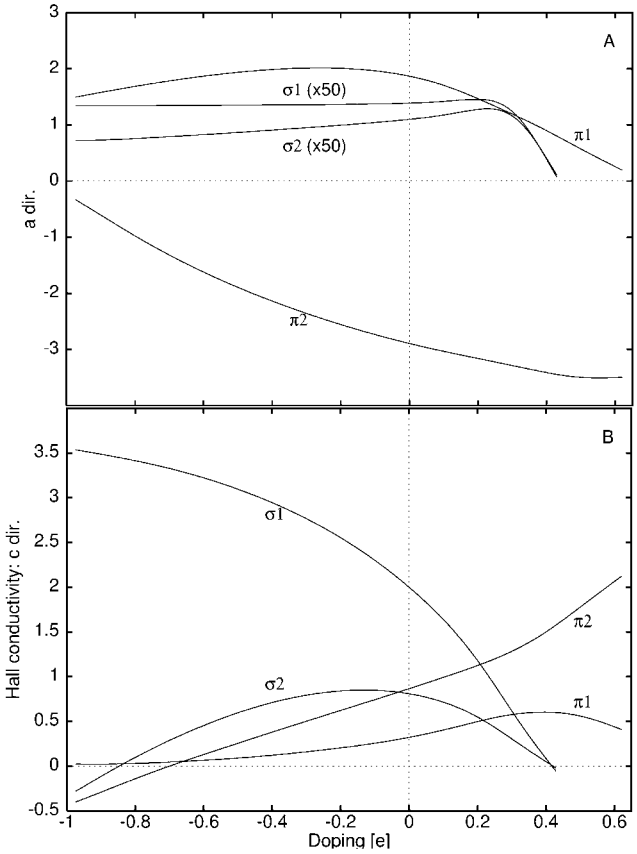

Figure 4. Hall conductivity factors ($\delta^n_{\mathrm{H}\gamma}$) for the different bands: (A) the magnetic field in the plane, (B) magnetic field in the c-direction. The σ-band contribution is very small in the a-direction, therefore the values in (A) are multiplied by 50.

Pinski *et al* 1981). These values strongly depend on the sample quality, which for the case of Putti *et al* was due to the purity of the chemical elements used. Their τ^σ_Q/τ^π_Q ratios for the different samples were 0.6 and 1.2.

In the $4\tau_{(\mathrm{opt})}$ curve of figure 2(A), the high temperature value (300 K) of Eltsev *et al* (2003) corresponds to $z = 0.127$ (equation (7)), which corresponds to $\tau^\sigma \approx 6.9\tau^\pi$. With $x \approx 2/3$, $y \approx 1$ all the relative relaxation times are found: $2\tau^{\sigma 1} \approx \tau^{\sigma 2} \approx 2.3\tau^{\pi 2} \gg \tau^{\pi l}$. For the particular case of $x = \frac{1}{2}$ ($\tau^{\sigma 1} = \tau^{\sigma 2}$) and $\tau^{\pi 2} \gg \tau^{\pi 1}$ only two effective relaxation times, $\tau^{\sigma 1}$ and $\tau^{\pi 2}$, would remain with $\tau^{\sigma 1} \approx 3.4\tau^{\pi 2}$.

The above discussion is based on:

(a) a single experimental result (Eltsev *et al* 2003), in which, as noted by Masui and Tajima (2003) the σ_c conductivity measurements are not very reliable (the ratio σ_a/σ_c is between 3 and 10), and
(b) an approximate Hall conductivity expression (equation (4) and the discussion that follows).

Consequently the results for the relaxation times cannot be taken as solidly founded. The explanation of the Hall anisotropy remains a challenge for both theorists and experimentalists and has to be considered an unsolved problem.

5.2. Al-doping

MgB_2 electron doping can be studied with the *rigid band approximation*, which consists in shifting E_F but leaving the band structure unchanged. This doping would resemble the effect associated of replacing Mg by Al. That is, since Al has one electron more, additional electrons are added to the system. Mg and Al are almost completely ionized in these compounds (de la Mora *et al* 2002); this replacement has little effect on the band structure, except for the position of E_F.

Satta *et al* (2001) have done a similar study in (Mg, Al)B_2, but in their treatment they worked with all the bands together and only one relaxation time τ, whereas in the present study the different bands are analysed separately and with different relaxation times. The results presented here (both the total conductivity and the Hall coefficient), using the same $\tau^n = \tau$ for all the bands, are in close agreement with those of Satta *et al* (they calculated the plasma frequency, which can be related to the conductivity using the equation (5)).

From the band structure plot (figure 1(B)) it can be seen that shifting down E_F the σ- and π-bands come closer in k-space (see Γ–M and Γ–K), therefore the corresponding Fermi surfaces also come closer and at ~ -1.2 eV the bands cross and the Fermi surfaces cannot be easily separated any more. On the other hand, raising E_F separates the σ- and π-surfaces; the σ-surfaces disappear at 0.82 eV.

The transport properties will be calculated in the $[-1.2, 1.5$ eV] range. The E_F shift is measured in eV, while doping is measured in electrons (e). The eV scale can be transformed to electrons using the density of states plot; the new range now becomes $[-0.97, 0.62$e] and the σ-band edge (0.82 eV) becomes 0.43e. In the Al fully-doped compound, AlB_2, the energy shift would be $\sim$2 eV (de la Mora *et al* 2002). The range will not be extended to 2 eV since new three-dimensional bands appear at $\sim$1.7 eV. These bands would unnecessarily complicate the analysis since at such high doping range the material is no longer superconducting (Bianconi *et al* 2002, Putti *et al* 2003a, Slusky *et al* 2001).

On increasing the doping (figures 1(A) and (B)) the σ tubular Fermi surfaces shrink towards the Γ–A line until they disappear at the band edge; therefore their contribution to the conductivity diminishes (and finally disappears). This is reflected in the conductivity calculations, figures 3(A) and (B). In the a-direction, $\sigma_a^{\sigma 1}$ and $\sigma_a^{\sigma 2}$ are very similar, and above E_F they are almost identical. For the c-direction ($\sigma_c^{\sigma 1}$, $\sigma_c^{\sigma 2}$) they are not so similar, but still they have the same trend; this is reflected in the $\sigma_a^{\sigma i}/\sigma_c^{\sigma i}$ ratio (figure 3(C)).

From figures 3(A) and (B) it can be observed that the $\pi 1$-band conductivity decreases as well, but it does not disappear, while for $\pi 2$ it increases. From this perspective, the $\sigma 1$-, $\sigma 2$- and $\pi 1$-bands are hole-like, while the $\pi 2$-band is electron-like. All the bands have contributions to the conductivity in the a-direction of the same order, while in the c-direction the σ-band contribution is much smaller, about 1/50 of the π-band contribution.

The σ-Hall conductivity factor $\delta_{Ha}^{\sigma n}$ is small, 1/50 of the π-band contribution (figure 4(A)). The $\sigma 1$, $\sigma 2$ and $\pi 1$ are all positive while $\pi 2$ is negative; that is, the former ones are hole-like and the latter one is electron-like, in agreement with the conductivity results above and those given by Masui and Tajima (2003). On the other hand, figure 4(B) shows that in δ_{Hc}^{n} all the contributions are of the same order, but all positive; that is, all are hole-like.

As a matter of comparison, for the cuprates the calculated a/c-ratio in the conductivity is of the same order as for the σ-bands on MgB_2. For example, for $La_{1.85}Sr_{0.15}CuO_4$ it is 27.5, for $YBa_2Cu_3O_7$ the a/c-ratio is 16 and for the b/c-ratio is 7 (Allen *et al* 1988). The experimental anisotropy is orders of magnitude larger (10^2–10^5). Additionally to this anisotropy, the temperature dependence of ρ_c is in most cases semiconducting, $d\rho_c/dT < 0$, whereas that of ρ_{ab} is metallic, $d\rho_c/dT > 0$. For MgB_2 both resistivities, ρ_a and ρ_c, are

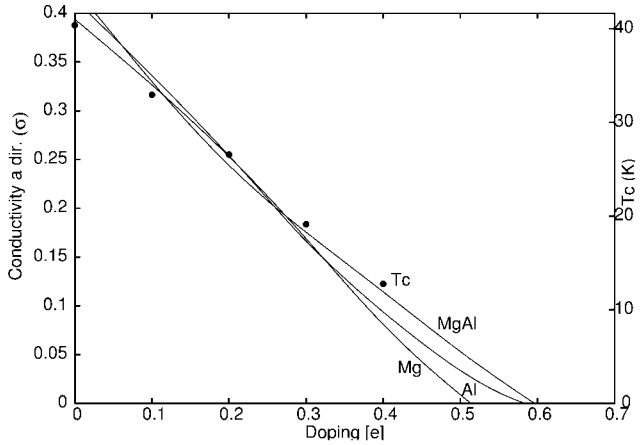

Figure 5. σ_a^σ for doped MgB_2, $Mg_{0.5}Al_{0.5}B_2$ and AlB_2 using the *rigid band approximation*, the horizontal axis was multiplied by 1.23. The experimental T_c-values of Putti *et al* are also plotted.

metallic. It is important to note that MgB_2 has a different superconductivity mechanism from the cuprates: it is very similar to the traditional *BCS* materials, although it is multiband.

As can be seen, the anisotropy in the conductivity is present in all high-T_c superconductors, including MgB_2. This last material seems to be in this category due to the fact, as was mentioned above, that superconductivity is sensitive to the band origin of the electrons; that is, the large superconducting gap is associated to the highly anisotropic σ-bands.

What will be analysed in the following sections is the σ-band conductivity for different compounds. Since the $\sigma 1$- and $\sigma 2$-bands have a very similar behaviour then it is not important what $\tau^{\sigma 1}/\tau^{\sigma 2}$ ratio is taken, and $\tau^{\sigma 1}$, $\tau^{\sigma 2}$ will be assumed to be equal ($\tau^{\sigma 1} = \tau^{\sigma 2}$).

From the results shown in figure 3, it can be seen that by increasing the electron doping the σ-band contribution diminishes and the anisotropy character of these bands also diminishes. Therefore the high-T_c superconductivity in this material should disappear with electron doping, since the main electron–phonon coupling is due to boron in-plane phonons (Yildirim *et al* 2001).

This can be more clearly observed when MgB_2 is doped with aluminium (Bianconi *et al* 2002, Putti *et al* 2003a, Slusky *et al* 2001); here T_c diminishes with the Al content. Putti *et al* (2003a) found a linear relationship between Al content and T_c: extrapolating T_c would reach 0 at ∼0.6Al. Bianconi *et al* (2001, 2002) found a similar relationship, but with a change of slope at 0.33Al and $T_c \to 0$ at ∼0.53Al. de la Peña *et al* (2002) could reproduce the results of Bianconi *et al* (2001), with the assumption that $T_c \sim$ number of σ-carriers. Our calculations for σ_a^σ diminishes almost linearly with a small downward curvature and vanishes at 0.43e (figure 3(A)).

5.3. Adjustment to the rigid band approximation

This small value, 0.43e, is due to the *rigid band approximation*; MgB_2, $Mg_{0.5}Al_{0.5}B_2$ and AlB_2 were calculated (the $Mg_{0.5}Al_{0.5}B_2$ compound was modelled with a supercell, alternating the Mg and Al layers in the *c*-direction), and with the *rigid band approximation* three parallel curves for σ_a^σ-conductivities were found. The σ_a^σ-values for MgB_2 are exact for zero doping; for $Mg_{0.5}Al_{0.5}B_2$ they are exact for 0.5e and for AlB_2 they are exact for 1e. Expanding the horizontal axis by 1.23, but keeping these σ_a^σ-values fixed (for instance, for $Mg_{0.5}Al_{0.5}B_2$ the axis is expanded to the left and to the right of 0.5e), the three curves overlap (figure 5).

The former change of scale from eV to doping (e) using the density of states appears to be naive, since other effects should be acting with Al-doping, such as charge transfer, and the relative positions of the σ- and π-bands change; by multiplying by 1.23 these effects seem to be taken into account, since now the three curves approximately match. With this adjustment of scale the *rigid band approximation* can be used to interpolate between these 0, $\frac{1}{2}$ and 1 doping-values. It is important to note that the *rigid band approximation* does not work so well for σ_c^σ, σ_a^π and σ_c^π. This is because these conductivities have a vertical component; σ_c^σ is the conductivity in the c-direction and is quite small ($\sim 1/50\sigma_a^\sigma$), therefore the change of Mg for Al should have an enlarged effect; for σ_a^π and σ_c^π there is a B:p_z orbital and the Al-doping has a direct effect. For σ_a^σ all is within the boron planes, and the change in conductivity just reflects the change of σ-carriers.

The experimental T_c-values of Putti *et al* are also plotted in figure 5; for these experimental values T_c closely follows σ_a^σ. It can also said that σ_a^σ follows the experimental values of Bianconi *et al* (2001, 2002), although the sharp drop at 0.33Al is not reproduced.

On the other hand, if this material could be doped with holes, such as in $(Na, Mg)B_2$, the opposite effect would be produced, and T_c should increase since σ_a^σ and the anisotropy increases; de Coss (2004) calculated the σ-Fermi surface area and they also predicted a rise of T_c when Na substitutes Mg in MgB_2.

5.4. Other compounds with AlB_2-structure

Satta *et al* (2001) and Medvedeva *et al* (2001) also calculated the band structure of BeB_2 (not a superconductor and an interesting compound to compare with) and found it to be very similar to MgB_2. There are important differences: (a) E_F is higher, closer to the σ-band edge, (b) the σ-band slope in the c-direction is significantly higher, while in other the directions it is similar. The first point (a) could be thought of as e-doping, as was discussed for aluminium (figure 2(A)), and the σ-conductivity should be lower; our calculations give $\sigma_a^\sigma(BeB_2) = 0.58\sigma_a^\sigma(MgB_2)$, and the second point (b) implies a lower anisotropy, (equation (6)); the calculations give $\sigma_a^\sigma/\sigma_c^\sigma = 7.5$ (for MgB_2: $\sigma_a^\sigma/\sigma_c^\sigma = 43$).

ScB_2, on the other hand, shows a low T_c ($\sim$1.5 K); this compound is similar to BeB_2 in relation to the σ-bands (Medvedeva *et al* 2001). The important difference is that Sc contributes with one d-electron. Our calculations show large changes in the morphology of the bands and Fermi surfaces. E_F is very close to the σ-band edge; that is, it is higher than in BeB_2, but it is not above the σ-band edge as in AlB_2. The σ-band slope in the c-direction is even higher than in BeB_2, and in this case the Fermi surfaces are almost spherical. The change in values is more drastic than in BeB_2: $\sigma_a^\sigma/\sigma_c^\sigma = 3.9$, $\sigma_a^\sigma(Sc) = 0.12\sigma_a^\sigma(Mg)$ (The Fermi surfaces were observed with XCrySDen, Kokalj 1999, using the output of WIEN2k).

The reduction of σ-carriers and the reduction of the σ-band anisotropy in BeB_2 and ScB_2 in comparison with MgB_2, could be important factors that may account for the large reduction of T_c.

ZrB_2, NbB_2 and TaB_2 have the same AlB_2 crystalline structure, but their electronic structure is quite different since they have several d-electrons, not just one as ScB_2. For instance, there are no anisotropic bands at E_F (de la Mora *et al* 2002), and the d-electrons add more charge to the compound, shifting E_F higher. Even more, the d-electrons also interact with the B:$p_{x,y}$ orbitals; that is, there are no pure B:σ orbitals anymore, as was the case for MgB_2. From the perspective of the present discussion these metallic borides are not expected to be high-T_c superconductors; TaB_2 is not a superconductor. For ZrB_2 Gasparov *et al* (2001) found $T_c = 5.5$ K (this result has not been confirmed by other experimental papers), and for NbB_2Escamilla *et al* (2004) found $T_c = 9.8$ K. The superconductivity of these materials may be originated from a different mechanism.

The anisotropy of the B:σ-bands in these AB_2 compounds, by itself, may not be responsible for the superconductivity, but it indicates the amount of contamination of the A-element orbitals. This contamination should also perturb the in-plane boron phonons, which probably become weaker. This shows the indirect influence of the anisotropy in the destruction of the superconductivity.

6. Conclusions

Conductivity measurements show that MgB_2 is a fairly isotropic conductor, but the fact that there are two superconducting gaps, one for the σ-bands and the other for the π-bands, gives a totally different perspective; that is, the electrons seem to distinguish which band they belong to. For this reason the different contributions to the electrical conductivity and Hall coefficients were analysed. This separation of contributions permitted the study of the individual band-anisotropy and their consequences on the transport properties. The σ-Fermi surfaces are very anisotropic, and the associated electrical conductivity is also anisotropic; in contrast, the π-Fermi surfaces are fairly isotropic.

In order to fit the experimental conductivity and Hall results, different relaxation times were needed, one for each band, with relative values $\tau^{\sigma 1}(=\tau^{\sigma 2}) \approx 3.4\tau^{\pi 2}(\gg\tau^{\pi 1})$.

The conductivity anisotropy measurements and theoretical Hall expressions are not yet accurate enough to obtain precise relative relaxation times τ^{α}. Therefore larger single crystals for transport properties measurements and better theoretically founded Hall expressions are needed.

The σ-band contributions and their conductivity anisotropy were discussed for several compounds in relation to the superconducting properties:

(a) ZrB_2, NbB_2 and TaB_2 have a low T_c or are non-superconducting; these materials do not have pure B:σ-band at E_F;
(b) BeB_2, a non-superconductor, and ScB_2, a low-T_c-superconductor, have E_F nearer the σ-band edge, also their bands are considerably less anisotropic;
(c) with Al-doping in $Mg_{1-x}Al_xB_2$ the experimental T_c reduces linearly with x; in our results σ_a^{σ} follows the same x-dependence; the σ-band anisotropy also diminishes with electron doping.

The σ-band contributions and their anisotropy emerge as fundamental factors that may play an important role in the superconducting mechanism of the MgB_2 system.

Acknowledgments

We thank the valuable suggestions of the referees. Support from DGAPA-UNAM under project PAPIIT-IN-101901 is gratefully acknowledged. Also support from María Sabina Ruiz-Chavarría was very valuable.

References

Allen P B 1987 *Phys. Rev.* B **36** 2920
Allen P B, Beaulac T P, Khan F S, Butler W H, Pinski F J and Swihart J C 1986 *Phys. Rev.* B **34** 4331
Allen P B, Pickett W E and Krakauer H 1987 *Phys. Rev.* B **36** 3926
Allen P B, Pickett W E and Krakauer H 1988 *Phys. Rev.* B **37** 7482
Allen P B and Schulz W W 1993 *Phys. Rev.* B **47** 14434
Ashcroft N W and Mermin N D 1976 *Solid State Physics* Holt-Saunders International Edn (Philadelphia, PA: Saunders) chapter 13
Bianconi A *et al* 2001 *J. Phys.: Condens. Matter* **13** 7382

Bianconi A *et al* 2002 *Phys. Rev.* B **65** 174515
Blaha P, Schwarz K, Madsen G K H, Kvasnicka D and Luitz J 2001 *WIEN2k, an Augmented Plane Wave + Local Orbitals Program for Calculating Crystal Properties* Karlheinz Schwarz, Techn. Universität Wien, Austria (ISBN 3-9501031-1-2)
Butler W H 1984 *Phys. Rev.* B **29** 4224
de Coss R 2004 personal communication
de la Mora P, Castro M and Tavizon G 2002 *J. Solid State Chem.* **169** 168 (In the last equation we made an error, which is corrected in the present paper, also the anisotropy value found of 4.74 was too high due to the small k-mesh and the integration procedure)
de la Peña O, Aguayo A and de Coss R 2002 *Phys. Rev.* B **66** 12511
Eltsev Y, Nakao K, Lee S, Masui T, Chikumoto N, Tajima S, Koshizuka N and Morakami M 2003 *J. Low Temp. Phys.* **131** 1069
Escamilla R *et al* 2004 *J. Phys.: Condens. Matter* **16** 5979
Eskildsen M R *et al* 2002 *Phys. Rev. Lett.* **89** 187003
Gasparov V A, Sidorov N S, Zver'kova I I and Kulakov M P 2001 *JETP Lett.* **73** 532
Hamada N, Massidda S, Jaejun Y and Freeman A J 1990 *Phys. Rev.* B **42** 6238
Iavarone M *et al* 2002 *Phys. Rev. Lett.* **89** 187002
Kokalj A 1999 *J. Mol. Graph. Model.* **17** 176
Reprinted figure with permission from, Kortus J, Mazin I I, Belashenko K D, Antropov V P and Boyer L L 2001 *Phys. Rev. Lett.* **86** 4656 (Copyright 2001 by the American Physical Society)
Liu A Y, Mazin I I and Kortus J 2001 *Phys. Rev. Lett.* **87** 087005
Masui T, Lee S, Yamamoto A and Tajima S 2002 *Physica* C **378–381** 216
Masui T and Tajima S 2003 *Physica* C **385** 91
Mazin I I and Antropov V P 2003 *Physica* C **385** 49
Medvedeva N I *et al* 2001 *Phys. Rev.* B **64** 20502 and references within
Nature, Physics Portal Highlights, May 2001 Available at www.nature.com/physics/physics.taf?file=/physics/highlights/6836-2.html
Perdew J P, Burke S and Ernzerhof M 1996 *Phys. Rev. Lett.* **77** 3865
Pinski F J, Allen P B and Butler W H 1981 *Phys. Rev.* B **23** 5080
Putti M, Affronte M, Manfrinetti P and Palenzona A 2003a *Phys. Rev.* B **68** 94514
Putti M *et al* 2003b *Phys. Rev.* B **67** 64505
Satta G, Profeta G, Bernardini F, Continenza A and Massida S 2001 *Phys. Rev.* B **64** 104507
Schmidt H *et al* 2002 *Phys. Rev. Lett.* **88** 127002
Schulz W W, Allen P B and Trivendi N 1992a *Phys. Rev.* B **45** 10886
Schulz W W *et al* 1992b *Phys. Rev.* B **46** 14001
Slusky J S, Rogado N, Regan K A, Hayward M A, Khalifah P, He T, Inumaru K, Louriro S M, Haas M K, Zandbergen H W and Cava R J 2001 *Nature* **410** 344
Szabó P *et al* 2001 *Phys. Rev. Lett.* **87** 137005
Yildirim T *et al* 2001 *Phys. Rev. Lett.* **87** 37001